Surface & Coatings Technology 206 (2011) 1336–1341

Contents lists available at SciVerse ScienceDirect

Surface & Coatings Technology

journal homepage: www.elsevier.com/locate/surfcoat

Spray deposited superhydrophobic ZnO coatings via seed assisted growth

N.L. Tarwal, V.M. Khot, N.S. Harale, S.A. Pawar, S.B. Pawar, V.B. Patil, P.S. Patil *

Thin Film Materials Laboratory, Department of Physics, Shivaji University, Kolhapur-416 004, Maharashtra, India

ARTICLE INFO

Article history:
Received 5 March 2011
Accepted in revised form 28 August 2011
Available online 2 September 2011

Keywords:
Zinc oxide thin films
Spray pyrolysis
Optical properties
Wettability

ABSTRACT

Superhydrophobic zinc oxide (ZnO) coatings were synthesized by a simple and cost-effective spray pyrolysis technique (SPT) via seed assisted growth onto the glass substrates at 723 K from an aqueous zinc acetate precursor solution. Initially, the ZnO seeds were synthesized from an aqueous 0.4 M zinc acetate solution onto the glass substrates at 723 K. For the seed assisted growth of ZnO, the solution concentrations (0.1 M to 0.4 M) were used and its effect on structural, morphological, optical and wettability properties of ZnO thin films was investigated. The synthesized films were found to be polycrystalline, with preferential growth along c-axis. Scanning electron microscopy (SEM) images show the uniform distribution of spherical grains of about 60–80 nm grain size. After seed assisted growth, film surface becomes very rough. The films were specular and transmittance of thin films decreases as the concentration of the precursor solution increases. The optical absorption spectrum shows a sharp absorption band-edge at 381 nm, corresponding to optical gap energy (Eg) of 3.25 eV. All samples are superhydrophobic in nature. The Zn4 sample shows the superhydrophobicity with highest value of the contact angle (CA) i.e. 165°. Such a superhydrophobic coatings can be useful in the anti-snow, anti-fog and self cleaning surfaces.

1. Introduction

Wettability is one of the most important properties of solid surfaces. It is influenced by both the surface energy and the geometrical microstructure of the surface. The wetting phenomena of water droplets on substrates are of crucial concern in our daily life as well as in engineering and science. Wetting CA between the liquid-gas (l-g) and liquid–solid (l–s) interfaces is used to characterize the nature of solid-fluid interactions [1]. Generally, a surface with water CA greater than 90° is referred as hydrophobic and one with water CA higher than 140° is qualified as ultra hydrophobic. The surfaces with very high water contact angles, particularly greater than 150°, are called as superhydrophobic surfaces, which have been extended to more number of applications. With the continuous developments of micro/nanotechnologies, researchers have investigated much about the state-of the-art microstructures from natural materials [2] and have been trying to find out approaches to mimic these natural materials. Some biological surfaces, like Lotus leaves, exhibit an amazing property of not being wetted by water, leading to a self-cleaning effect. Their surface roughness is generally composed of micro and nanostructures, creating a sort of carpet on which water droplets show a quasi-spherical shape [3,4]. Inspired from the Lotus leaf properties i.e. surfaces with high droplet mobility or self-cleaning surfaces, many studies have been conducted to prepare the superhydrophobic surfaces by adopting their novel ideas/routes: chemical modification of rough surfaces with low-energy molecules or roughening hydrophobic surfaces, different particle size deposition and patterning materials with micro- and nanotechnology tools [5–18].

Control over surface hydrophobicity is highly desirable and it has become an area of increasing investigation in recent years, due to the wide range of possible applications. Artificial superhydrophobic surfaces have received much attention due to their importance in fundamental research and promising applications [19], since they allow the design of self-cleaning and water-repellent surfaces with high water contact angles and low contact angle hysteresis [20]. The superhydrophobic surfaces with self-cleaning property has received much interests because of their applications in preventing the adhesion of water and snow to windows or antennas as well as for self-cleaning utensils, antioxidation coating, microfluidic devices, textile, microelectromechanical systems (MEMS) and lab-on-chip (LOC) or micro total analysis systems (μTAS) [21,22].

Over the past few years, many methods such as thermal evaporation [8], sol–gel technique [17], chemical bath deposition [23], hydrothermal [24], molecular beam epitaxy [25], sputtering [26], chemical vapour deposition [27], pulsed laser deposition [28], plasma etching [29], utilization of templates [30], SPT [15,16,31] and layer-by-layer deposition method [32], etc. have been employed to synthesize nanostructured ZnO thin films. Among all these methods, SPT has the advantages of low cost, easy-to-use, safe and can be implemented in a standard laboratory. Due to the simplicity of the apparatus and good productivity of this technique on a large scale, it offers a most attractive way for the formation of thin films, as demonstrated by Patil in his review [33].

* Corresponding author. Tel.: +91 231 2609230; fax: +91 231 2691533.
E-mail address: psp_phy@unishivaji.ac.in (P.S. Patil).

0257-8972/$ – see front matter © 2011 Elsevier B.V. All rights reserved.
doi:10.1016/j.surfcoat.2011.08.050

In our earlier research work [31], we have reported the superhydrophobic as well as transparent coatings with highest water CA 154°. Our main aim is to increase the CA value by adopting some novel route i.e. seed assisted growth, which is capable of creating conducive surfaces. In the present investigation, we report the improvement in the CA value of superhydrophobic ZnO coatings, which are deposited onto the glass substrates at fixed substrate temperature of 723 K by using SPT via seed assisted growth. The structural, morphological, optical and wettability properties of coatings at various concentrations (0.1 M to 0.4 M) were also investigated.

2. Experimental

To grow uniform thin film over the entire surface of the substrate, cleaning of the substrates is very important. Commercially available glass microslides were dipped in preheated chromic acid at 363 K for 15 min, washed with laboline, rinsed in acetone and finally, ultrasonically cleaned with double distilled water for 15 min prior to the actual deposition of the ZnO coatings.

Initially, ZnO seeds were synthesized using SPT onto the ultrasonically cleaned glass substrates from 0.4 M aqueous zinc acetate precursor solution. The resulting solution was then further pulverized pneumatically by means of a specially designed glass nozzle onto the preheated glass substrates. The sprayed droplets undergo evaporation, solute condensation and thermal decomposition, thereby resulting in the formation of ZnO coatings. The synthesized seed sample is denoted by Zn0. Further, the seed samples were utilized for the seed assisted growth of ZnO thin films. For this growth, the precursor solution of various concentrations from 0.1 M to 0.4 M was used as a spraying solution and deposited thin film samples are denoted as Zn1, Zn2, Zn3, Zn4, respectively. During the thin film synthesis, various preparative parameters of the SPT like solution concentration (0.4 M), solution quantity (40 cc), spray rate (5 cc min^{-1}), nozzle to substrate distance (22 cm), carrier gas (compressed air), etc. were optimized to obtain uniform, adhesive and pin hole free deposits. The substrate temperature was kept constant at 723 K for the all depositions.

Film thickness and roughness of all the deposited samples were measured by Ambios XP-1 surface profiler. The structural and morphological characterizations were carried out using Philips PW 3710 X-ray diffractometer with CuKα radiation (wavelength 1.5405 Å) and scanning electron microscope JEOL JSM-6360 model, respectively. The optical characterizations were carried out using UV–Vis Systronics spectrophotometer over the wavelength range 350 to 750 nm. The wettability of the ZnO films was examined by means of the water CA using a contact angle meter (Rame-Hart 500-F1-USA) at ambient temperature.

3. Results and discussion

3.1. Thickness and roughness

Fig. 1 shows the plot of thickness and roughness of all the seed assisted ZnO films with respect to the concentration of the precursor solution. The film thickness and roughness of the samples are increased from 860 to 1024 nm and 85 to 110 nm, respectively. The increase in the film thickness is due to the active mass deposited onto the substrate at higher concentration of the precursor solution.

3.2. Structural properties

The structural changes and identification of phases were investigated with the help of X-ray diffraction (XRD) technique. Fig. 2 shows the XRD patterns recorded over 10°-100° for the Zn0, Zn1, Zn2, Zn3 and Zn4 samples deposited onto the glass substrates at 723 K. All relatively sharp diffraction peaks can be well assigned to the hexagonal-phase, reported in the literature [34]. From XRD patterns, it is clear that deposited ZnO films are highly oriented along (002) plane. Other orientations

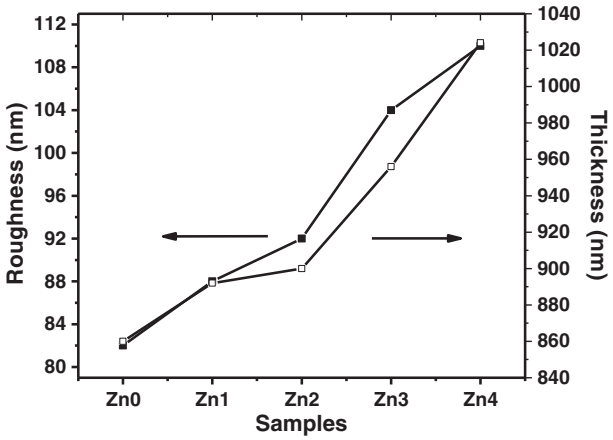

Fig. 1. Plot of thickness and roughness of all seed assisted growth of ZnO thin films.

corresponding to (100), (101), (102), (103), (112) and (004) planes are present with low relative intensities as compared to that of (002) plane, indicating the preferred growth direction along c-axis. No peaks other than ZnO were detected, which confirms the pure phase of ZnO.

The initial seed sample (Zn0) was found to be less crystalline. For the seed assisted ZnO samples, the intensity of (002) plane is increased progressively as the concentration of the precursor solution increases. Increase in (002) diffraction peak intensity is due to increased film thickness and preferred orientation. The film's crystalline properties are characterized by the crystallite size. The crystallite size was calculated by using the well-known Debye–Scherrer's formula as shown in Eq. (1) and the calculated values of the crystallite size are given in the Table 1.

$$D = \frac{0.9\lambda}{\beta \cos\theta} \tag{1}$$

where, λ is the wavelength (1.5406 Å) and β is full width in radian at half maximum of the peak and θ is the Bragg's angle of the XRD peak. The crystallite size increases from 40 nm to 45 nm, which indicates the slight improvement in the crystallinity. Among the all studied samples, the Zn4 sample shows the highest crystalline quality. Similar results were reported by Shinde et al. [35] and Joseph et al. [36] for spray deposited ZnO thin films from aqueous medium.

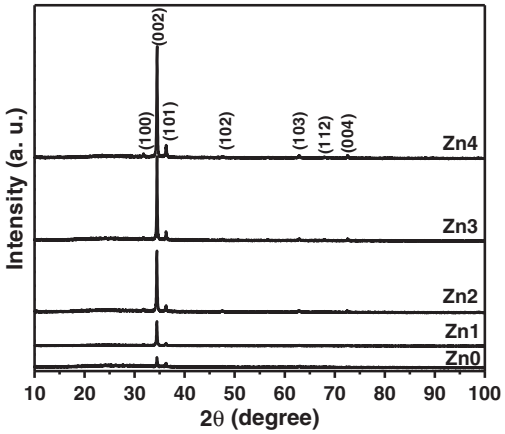

Fig. 2. XRD patterns of ZnO: Zn0, Zn1, Zn2, Zn3 and Zn4 thin films.

Table 1
Calculated crystallite sizes of the spray deposited superhydrophobic coatings (Zn0–Zn4 samples) at different concentrations (0.1 M–0.4 M).

Sample code	Crystallite size (nm)
Zn0	40
Zn1	42
Zn2	43
Zn3	44
Zn4	45

3.3. Morphological properties

The morphology of the ZnO thin films was checked by using scanning electron microscope. Typical SEM images (×20,000 magnification) of Zn0, Zn1, Zn2, Zn3 and Zn4 samples deposited at 723K onto the glass substrates, are shown in Fig. 3. During the pyrolytic decomposition of the precursor solution onto the preheated glass substrates, different atomic rearrangement processes involved which are responsible for the different surface topographies of the thin films. The SEM micrographs show that the surface morphology of the films is strongly dependent on the solution concentration.

The seed sample (Zn0) shows the uniform distribution of tiny spherical grains with compact and smooth morphology. For 0.1 M (Zn1 sample), the surface with non-uniform distribution of the spherical grains is observed. At 0.2 M solution concentration the films become relatively more compact and uniform with tiny crystallites. The grain growth due to the agglomeration, coalescence and aggregation events during the deposition at 0.3 M causes roughness of the Zn3 film to increase. These events occur more vigorously at higher concentration and subsequently cause the increment in its asperity for Zn4 sample. This behavior is consistent with Shinde et al. [35], who observed that increase in the grain size with an increase in the concentration of the sprayed precursor solution.

3.4. Optical properties

Optical properties of the material play a vital role in the device fabrication. The optical absorption spectra of all the ZnO thin films were recorded over the wavelength range 350–750 nm at room temperature are shown in Fig. 4. It is found that absorption of the films increases with solution concentration. Also it is observed that, the absorption edge at 380 nm is slightly shifted towards the higher wavelength. The optical band gap energy of ZnO thin films was

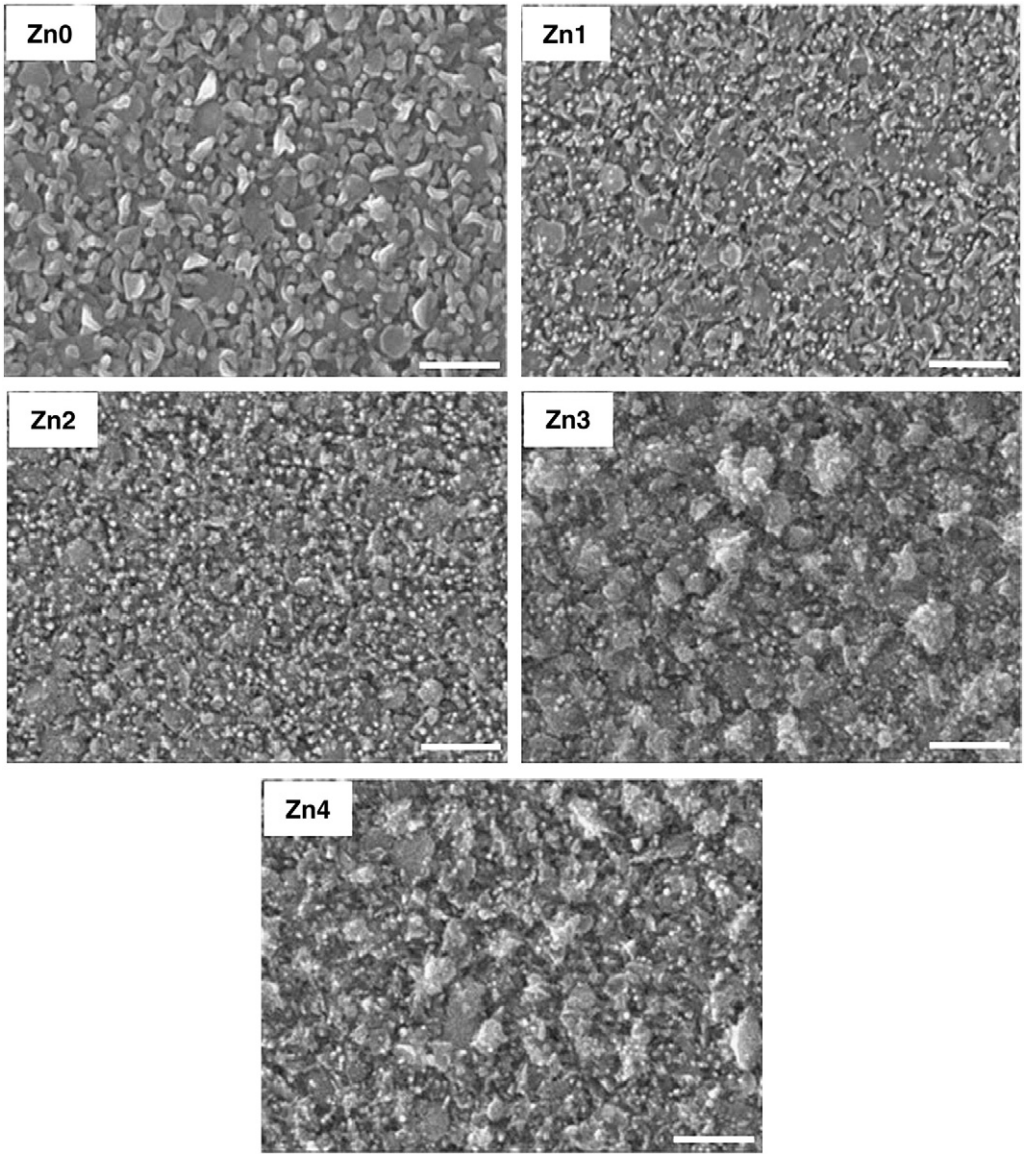

Fig. 3. SEM images of ZnO: Zn0, Zn1, Zn2, Zn3 and Zn4 thin films (scale bar = 1 μm).

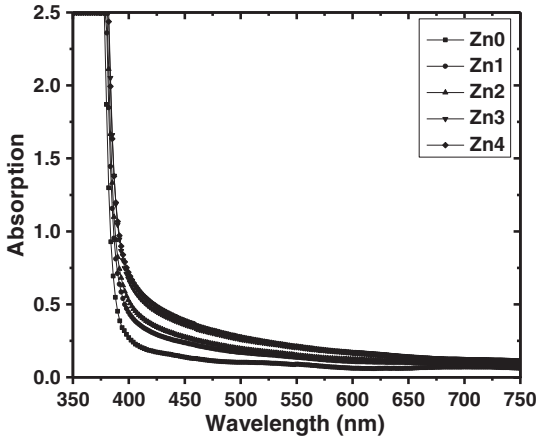

Fig. 4. Absorption spectra of ZnO: Zn0, Zn1, Zn2, Zn3 and Zn4 thin films.

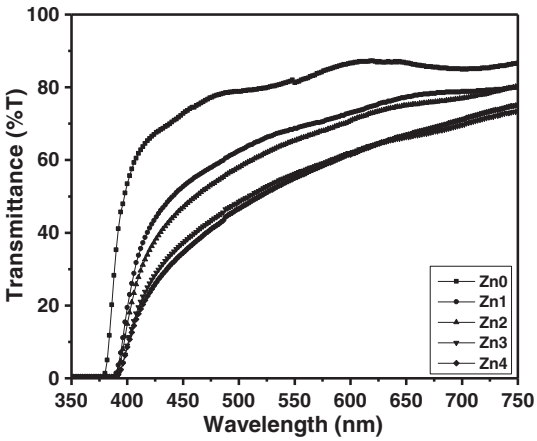

Fig. 6. Transmittance spectra of the ZnO: Zn0, Zn1, Zn2, Zn3 and Zn4 thin films.

estimated from optical absorption measurement. The optical absorption data were analyzed using the following classical relation (2) of optical absorption in semiconductor near band edge [37].

$$\alpha = \frac{\alpha_0(h\upsilon - Eg)^n}{h\upsilon} \tag{2}$$

where, Eg is the separation between bottom of the conduction band and top of the valence band, hν is the photon energy and n is a constant. Thus, if plot of $(\alpha h\nu)^2$ versus $(h\nu)$ is linear the transition is direct allowed. Extrapolation of the straight-line portion to zero absorption coefficient ($\alpha = 0$), leads to estimation of band gap energy (Eg) values. Fig. 5 shows variation of $(\alpha h\nu)^2$ as a function of photon energy $(h\nu)$. From Fig. 5, it is observed that all the samples show direct allowed transition and the inset of the Fig. 5 shows that, the optical band gap energy is decreases from 3.23 to 3.18 eV for the samples Zn0 to Zn4, respectively. The observed band gap energy values are in good agreement with the results reported by others [38].

The recorded transmittance spectra for all the ZnO films are shown in Fig. 6. The transmittance of the seed sample (Zn0) is about 85%. It is found that, the transmittance of the seed assisted ZnO films decreases as the solution concentration increases. The decrease in transmittance with an increase in concentration of the precursor solution can be explained as follows. As the concentration of solution increases, film growth increases which in turn, increases the film thickness. The less transmittance for Zn4 sample is due to the more active mass deposited on glass substrate from higher solution concentration (0.4 M). Also, it is related to the higher roughness of the films. The rough surface causes the more scattering because of which the transmittance of the films is decreases.

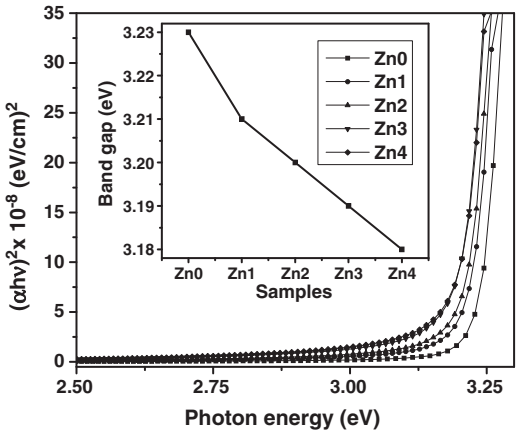

Fig. 5. Band gap energy of the ZnO: Zn0, Zn1, Zn2, Zn3 and Zn4 thin films. (Inset shows the variation with samples deposited from 0.1 M–0.4 M solution concentrations).

3.5. Contact angle measurements

The classical way to make advancing and receding angle measurements is to tilt the sample until the drop just begins to roll downhill. When a liquid drop is moved on a solid, the contact angle ahead (advancing) of the drop is usually larger than the contact angle at rear (receding); this phenomenon which occurs for nonwetting liquids is given the name of CA hysteresis. The very important property, wettability involves the interaction between liquid and solid in contact. It is known that, the wettability of an ideal surface, expressed by the CA (θ) of water droplets, is given by Young's Eq. (3):

$$\cos\theta = \frac{(\gamma_{SV} - \gamma_{SL})}{\gamma_{LV}} \tag{3}$$

where, γ_{SV}, γ_{SL} and γ_{LV} refer to the interfacial surface tensions with solid-vapor, solid-liquid and liquid-vapor, respectively. Young's angle is a result of the thermodynamic equilibrium of the free energy at the solid–liquid–vapor interphase.

In general, surface roughness is considered to be the key factor affecting surface wettability [14,31]. The wettability of a surface can be enhanced by increasing the surface roughness within a special size range because the air trapped between the solid surface and the water droplet can minimize the contact area. The relationship between the surface wettability and the surface roughness can be well described by the Cassie Eq. (4) [39]:

$$\cos\theta_r = f_1 \cos\theta - f_2 \cos\theta_r \tag{4}$$

where, θ_r and θ are the CAs on ZnO with rough and smooth surfaces, respectively. f_1 and f_2 are the fractional interfacial areas of ZnO and the air trapped between the ZnO surface and a water droplet, respectively (i.e. $f_1 + f_2 = 1$). This equation indicates that the larger air fraction ($f2$), the more hydrophobic the surface.

The CA is an important parameter in surface science and its measurement provides a simple and reliable method for the understanding of surface energies. Both superhydrophilic and superhydrophobic surfaces are important for different practical applications. Dedova et al. [15] reported the morphology dependent wetting properties of ZnO thin films by spray pyrolysis with CA values in between 11 and 56°. Conversely, Sun et al. [16] reported the hydrophobic behaviour for flat surface of ZnO thin films synthesized by SPT having CA 109°. These reports clearly show that the superhydrophobicity is the surface dependent properties of the material.

In the present case, all seed assisted samples are superhydrophobic in nature (Fig. 7) with CA value larger than CA of the seed sample (Zn0) i.e. 154°. Fig. 8 shows the plot of CA of the samples with respect to concentration of the precursor solution. It is observed that, the superhydrophobicity of the sample increases with increase in solution concentrations. The increased superhydrophobicity of the samples has been attributed to the increase in the roughness of the samples. Among the studied precursor concentrations, the film prepared at 0.4 M concentration (sample Zn4), the fraction of the solid surface in contact with the water droplet is very less; because of its high rough surface, so it shows a highest degree of hydrophobicity with CA 165°, which is supported by the Cassie–Baxter model [40].

4. Conclusions

In conclusion, superhydrophobic ZnO thin films were deposited on glass substrates at 723K by using a simple and inexpensive pneumatic SPT from an aqueous zinc acetate solution via seed assisted growth. The superhydrophobicity can be modified merely by using the seed assisted growth and varying the concentration of the precursor solution. Subsequently, the effect of solution concentration on the surface roughness and wettability has been studied and their relation is derived. It is observed that, the sample which has the roughness value above 75 nm exhibits superhydrophopbicity. The deposited films were polycrystalline with preferred orientation along (002)

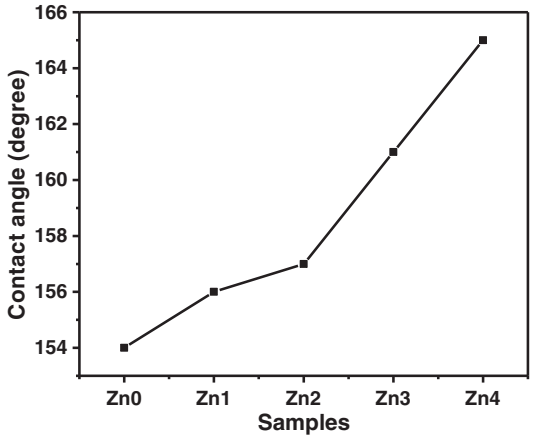

Fig. 8. Plot of variation of the contact angle with seed assisted growth of ZnO thin films.

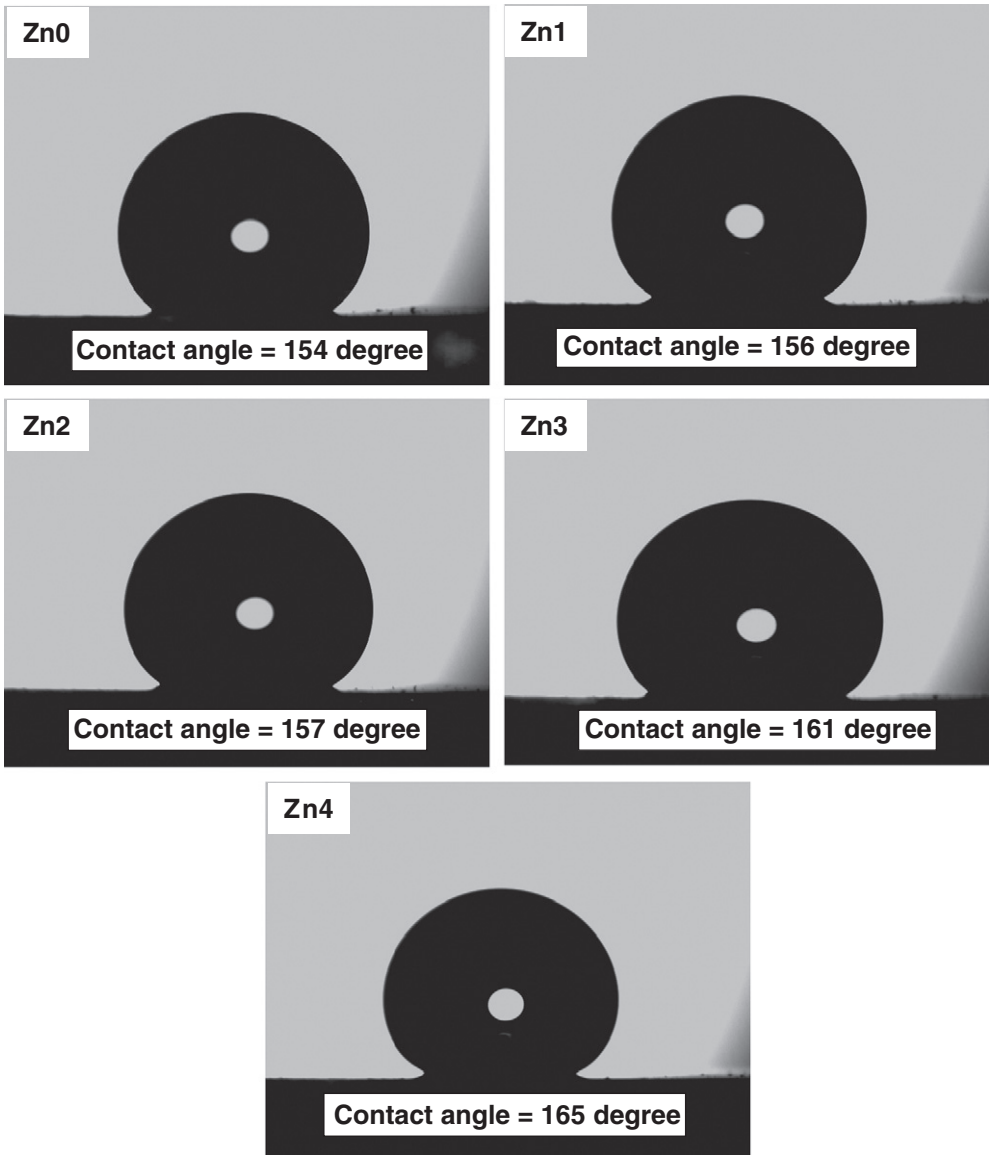

Fig. 7. Water contact angle of the ZnO: Zn0, Zn1, Zn2, Zn3 and Zn4 thin films.

plane in all the cases. The smooth and compact surface morphology with tiny spherical grains of the grain size 60–80 nm, was observed for seed (Zn0) sample. For the seed assisted samples (Zn1–Zn4), the surface becomes very rough. The observed band gap energy value of the films ranges from 3.23 to 3.18 eV. The transmittance of the films decreases as the concentration of the precursor solution increases. Among the studied samples, the seed assisted film prepared at 0.4M concentration (Zn4 sample) shows superhydrophobic nature with highest contact angle (165°). This area will hold an immense assurance in designing and developing bioanalytical methods, smart windows, microfluidic devices, biochips, environmental cleanup, controllable drug release and intelligent devices.

Acknowledgement

Authors wish to acknowledge the University Grants Commission (UGC), New Delhi, India for the financial support through the UGC-DRS-II phase, ASIST programmes and the Department of Science and Technology through DST-FIST programme. One of the authors NLT is thankful to University Grants Commission, New Delhi, for awarding the "Research Fellowship in Science for Meritorious Students to Promote Quality Research in Universities" under the UGC-DRS (SAP)–II programme.

References

[1] F.-M. Chang, Y.-J. Sheng, H. Chen, H.-K. Tsao, Appl. Phys. Lett. 91 (2007) 094108.
[2] A. Lafuma, D. Quere, Nat. Mater. 2 (2003) 457.
[3] B. Bhushan, Y.C. Jung, J. Phys, Condens. Matter 20 (2008) 225010.
[4] W. Xu, H. Liu, S. Lu, J. Xi, Y. Wang, Langmuir 24 (2008) 10895.
[5] S. Wang, Y. Song, L. Jiang, J. Photochem, Photobiol. C: Photochem. Rev. 8 (2007) 18.
[6] S. Patra, S. Sarkar, S.K. Bera, R. Ghosh, G.K. Paul, J. Phys. D: Appl. Phys. 42 (2009) 075301.
[7] X. Feng, L. Feng, M. Jin, J. Zhai, L. Jiang, D. Zhu, J. Am. Chem. Soc. 126 (2004) 62.
[8] X. Wu, P. Jiang, W. Cai, X.-D. Bai, P. Gao, S.-S. Xie, Adv. Eng. Mater. Commun. 10 (2008) 476.
[9] X. Hong, X.F. Gao, L. Jiang, J. Am. Chem. Soc. 129 (2007) 1478.
[10] M.H. Jin, X.J. Feng, L. Feng, T.L. Sun, J. Zhai, T.J. Li, L. Jiang, Adv. Mater. 17 (2005) 1977.
[11] X.Y. Song, J. Zhai, Y.L. Wang, L.J. Jiang, Phys. Chem. B 109 (2005) 4048.
[12] M. Guo, P. Diao, S. Cai, Thin Solid Films 515 (2007) 7162.
[13] N.S. Pesika, Z. Hu, K.J. Stebe, P.C. Searson, J. Phys. Chem. B 106 (2002) 6985.
[14] Y. Li, M. Zheng, L. Ma, M. Zhong, W. Shen, Inorg. Chem. 47 (2008) 3140.
[15] T. Dedova, J. Klauson, C. Badre, Th. Pauporté, R. Nisumaa, A. Mere, O. Volobujeva, M. Krunks, Phys. Stat. Sol. A 205 (2008) 2355.
[16] R.D. Sun, A. Nakajima, A. Fujishima, T. Watanabe, K. Hashimoto, J. Phys. Chem. B 105 (2001) 1984.
[17] X. Wu, L. Zheng, D. Wu, Langmuir 21 (2005) 2665.
[18] X.T. Zhang, S. Sato, A. Fujishima, Langmuir 20 (2004) 6065.
[19] D. Quere, Rep. Prog. Phys. 68 (2005) 2495.
[20] Y. Xiu, S. Zhang, V. Yelundur, A. Rohatgi, D.W. Hess, C.P. Wong, Langmuir 24 (2008) 10421.
[21] X. Gao, L. Jiang, Nature 432 (2004) 36.
[22] R. Blossey, Nat. Mater. 2 (2003) 301.
[23] K.V. Gurav, V.J. Fulari, U.M. Patil, C.D. Lokhande, O.S. Joo, Appl. Surf. Sci. 256 (2010) 2680.
[24] J.X. Wang, X.W. Sun, Y. Yang, H. Huang, Y.C. Lee, O.K. Tan, L. Vayssieres, Nanotechnology 17 (2006) 4995.
[25] D.M. Bagnall, Y.F. Chen, Z. Zhu, T. Yao, S. Koyama, M.Y. Shen, T. Goto, Appl. Phy. Lett. 70 (1997) 2230.
[26] Y. Nagoya, B. Sang, Y. Fujiwara, K. Kushiya, O. Yamasec, Sol. Energy Mater. Sol. Cells 75 (2003) 163.
[27] V. Sallet, C. Thaindoume, J.F. Rommeluere, A. Kusson, A. Riviere, J.P. Riviere, O. Gorochov, R. Triboulet, V.M. Sanjose, Mater. Lett. 53 (2002) 126.
[28] Y.R. Ryu, W.J. Kim, H.W. White, J. Cryst. Growth 219 (2000) 419.
[29] M.H. Jin, X.J. Feng, J.M. Xi, J. Zhai, K. Cho, L. Feng, L. Jiang, Macromol. Rapid Commun. 26 (2005) 1805.
[30] J. Li, J. Fu, Y. Cong, Y. Wu, L.J. Xue, Y.C. Han, Appl. Surf. Sci. 252 (2006) 2229.
[31] N.L. Tarwal, P.S. Patil, Appl. Surf. Sci. 256 (2010) 7451.
[32] J.T. Han, Y. Zheng, J.H. Cho, X. Xu, K. Cho, J. Phys. Chem. B 109 (2005) 20773.
[33] P.S. Patil, Mater. Chem. Phys. 59 (1999) 185.
[34] H. Gomez, M. de la L Olvera, Mater. Sci. Eng. B 134 (2006) 20.
[35] V.R. Shinde, T.P. Gujar, C.D. Lokhande, Sens. Actuators B 120 (2007) 551.
[36] Joseph Benny, P.K. Manoj, V.K. Vaidyan, Ceram. Inter. 32 (2006) 487.
[37] R.K. Pandey, S.N. Sahu, S. Chandra, Handbook of Semiconductor Electrodeposition, Marcel Dekker, Inc., New York, 1996, p. 142.
[38] B.J. Lokhande, M.D. Uplane, Appl. Surf. Sci. 167 (2000) 243.
[39] A.B.D. Cassie, Discuss. Faraday Soc. 3 (1948) 11.
[40] A.B.D. Cassie, S. Baxter, Trans. Faraday Soc. 40 (1944) 546.